ANNALI DI GEOFISICA, VOL. 42, N. 4, August 1999

A review of nonparametric attenuation functions computed for different regions of Italy

Raúl R. Castro ([1]), **Marco Mucciarelli** ([2]), **Giancarlo Monachesi** ([3]), **Francesca Pacor** ([4]) **and Raniero Berardi** ([5])

([1]) *División Ciencias de la Tierra, CICESE, Baja California, México*

([2]) *Università della Basilicata, Potenza, Italy*

([3]) *Osservatorio Geofisico Sperimentale di Macerata, Italy*

([4]) *ISMES, Divisione Geofisica, Bergamo, Italy*

([5]) *Ente Nazionale per l'Energia Elettrica (ENEL), Roma, Italy*

Abstract

We used a set of previously published nonparametric attenuation functions to calculate average functions for the Italian region. These nonparametric functions describe the spectral amplitude decay of the *S* waves as a function of distance for 14 frequencies between 1 and 20 Hz for the regions of Lombardia-Piemonte, Eastern Sicily, Friuli, Marche and the Central Apennines. Since all the attenuation functions were obtained using the same methodology, we were able to make a fair comparison of the attenuation characteristics of the different regions. In general, while the Central Apennines show the strongest amplitude decay for all the frequencies analyzed, the regions of Lombardia and Eastern Sicily show the smallest attenuation. The Marche region also shows a strong amplitude decay, particularly for frequencies $f > 3$ Hz, and in the frequency band between 1 and 3 Hz the rate of decay of the spectral amplitudes with distance becomes similar to that of the region of Friuli. Since the attenuation functions analyzed represent different geologic and tectonic environments, we used them to calculate an average set of attenuation functions, one per frequency, for the hypocentral distance range between 10 and 120 km. The resulting functions permit a mean attenuation correction to spectral records of *S* waves in regions of Italy where the specific values of the attenuation parameters are unknown.

Key words *seismic attenuation – S waves – nonparametric inversion – acceleration spectra*

1. Introduction

Recent estimates of the spectral amplitude decay of *S* waves found for different regions of Italy provide a good opportunity to compare the attenuation characteristics of regions with different geologic features. Although the attenuation of seismic waves can be characterized with the quality factor Q and the geometrical spreading, because of the trade-off between these parameters, a straight comparison of seismic attenuation between different regions, using only Q, may lead to inconsistent conclusions. Another complication is that the estimates of Q also depend on the type of waves and method used to separate source and path effects. An alternative approach to analyze the attenuation of seismic waves is to find nonparametric functions that describe the amplitude decay with distance (*e.g.*, Brillinger and Preisler, 1984; Anderson and

Mailing address: Dr. Raúl R. Castro, CICESE, Division Ciencias de la Tierra, Apartado Postal 2732, Ensenada, Baja California, 22860, México; e-mail: raul@cicese.mx

Quaas, 1988; Castro *et al.*, 1990; Anderson and Lei, 1994). In this paper we compare Nonparametric Attenuation functions (hereafter referred to as NAF) previously obtained by Castro *et al.* (1993) for the regions of Lombardia, Piemonte and Eastern Sicily, and by Castro *et al.* (1996, 1999a,b) for the regions of Friuli, Marche and the Central Apennines, respectively. In these studies the attenuation functions were obtained using spectral amplitudes of *S* waves at the same frequencies for all the regions and using the same methodology.

In the first section of this paper we make a brief review of the method used to derive the NAF of the different regions, then we describe the characteristics of the data used, and finally, we discuss the possible causes of the different attenuation characteristics inferred by comparing the reported NAF.

2. Method

For all the data sets used, except for the Umbria-Marche data sets, we calculated acceleration spectra of the *S* waves selecting time windows starting with the first *S* wave arrival and ending when 85% of the total energy of the record was reached. This criterion was used to include only *S*-wave energy in the windows. To avoid surface wave contamination, we used only 80% of the total energy for the records from the Central Apennines. For the data set from the Marche the windows were selected manually. The window lengths of this data set vary between 3 and 7 s, which represent at least 80% of the *S*-wave energy of the record. The time series were baseline corrected and cosine tapered. Then the acceleration spectra were instrument corrected and smoothed around pre-selected frequencies. In this paper we will analyze only the results found in the frequency band between 1 and 20 Hz (14 frequencies). The frequency band useful for analysis was selected by visual inspection of the spectral records using semi-logarithmic plots. The frequency at which the spectra became flat was chosen as the end of the signal. For many records this frequency was at about 25 Hz (*e.g.*, Castro *et al.*, 1996). The signal to noise ratio was also analyzed calculating the Fourier transform of a time window preceding the *P*-wave arrival (Castro *et al.*, 1993, 1999b). Since for Eastern Sicily the strong motion instruments triggered with the arrival of the *S* wave, the noise window was selected at the end of the *S*-wave coda. In general, the signal to noise ratio is a factor greater than 2 in the frequency band of the analyses (1 to 20 Hz). This ratio tends to increase for $f > 1.0$ Hz and then decreases for $f > 10$ Hz.

For each frequency f, the decay of the spectral amplitudes with hypocentral distance r is described by a nonparametric function $A(r,f)$ which is constrained to be a smooth decreasing function of r with a value of one at distance zero (*e.g.,* Anderson and Quaas, 1988; Castro *et al.*, 1990, 1996). Thus, the observed acceleration spectral amplitudes $U_i(r,f)$ are modeled as

$$U_i(r,f) = S_i \cdot A(r,f) \qquad (2.1)$$

$A(r,f)$ is obtained by linearizing eq. (2.1) and inverting for the S_i scalar (one for each earthquake i) and discrete values of the attenuation function. In this approach, the site effect is eliminated with the smoothing constraint. However, the site response $Z(f)$ of a given station j can be estimated as

$$Z_j(f) = \frac{U_{ij}(r,f)}{S_i \cdot A(r_j, f)}. \qquad (2.2)$$

In eq. (2.1), the NAF are not limited to have a specific functional form and it is also assumed that they implicitly contain the effects of both Q and geometrical spreading.

3. Data

3.1. *Region of Lombardia-Piemonte*

The Lombardia-Piemonte region extends from the Southern Alps to the Po basin (see fig. 1). The western structures of the Alps are the result of the interaction of the European and the Adriatic plates (Spakman *et al.*, 1993; Marchant, 1993).

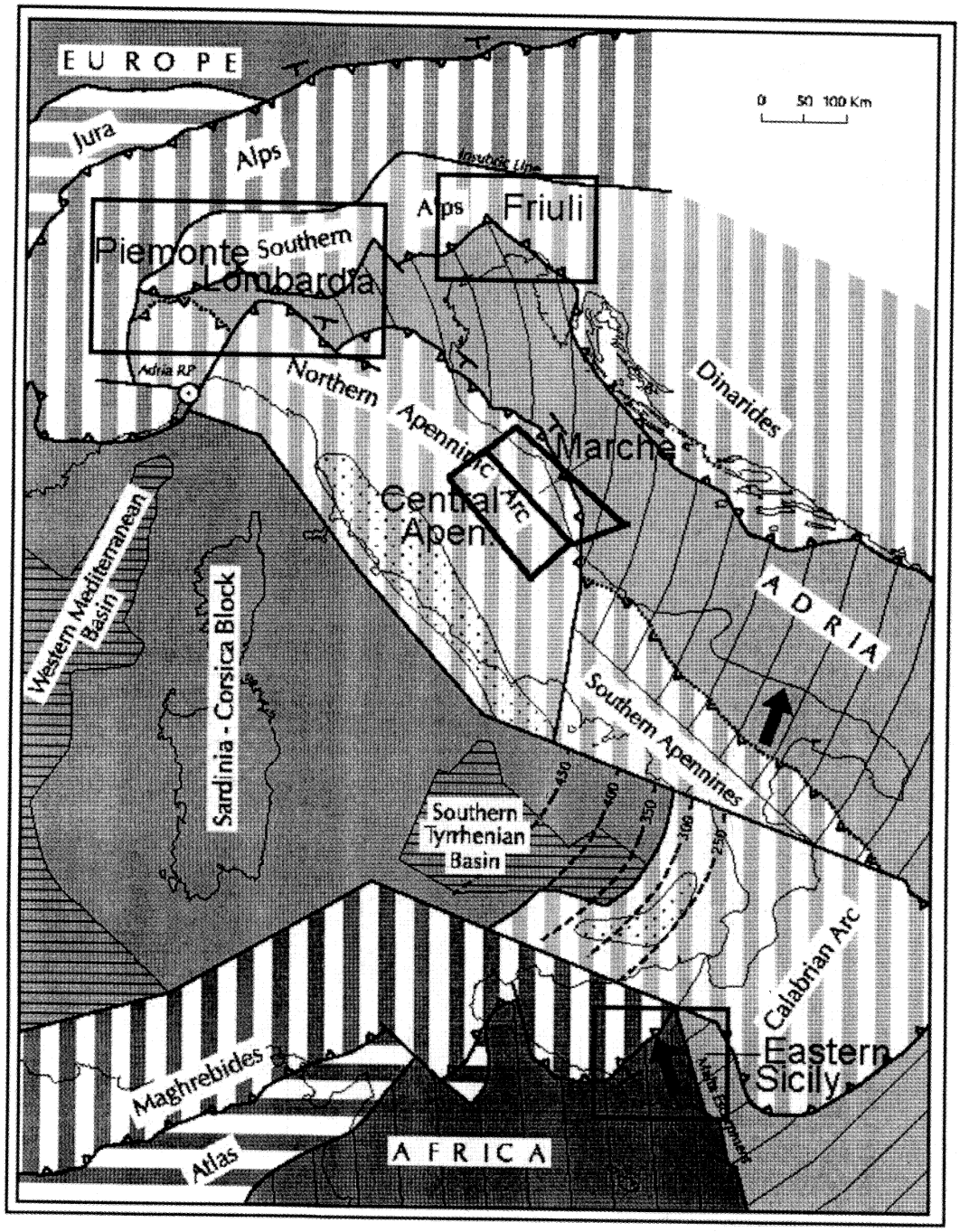

Fig. 1. Sketch of the main tectonic units of Italy with superimposed areas mentioned in this study. This figure was taken and modified from the original at the web site http://emidios.itim.mi.cnr.it/GNDT/P511/home.html

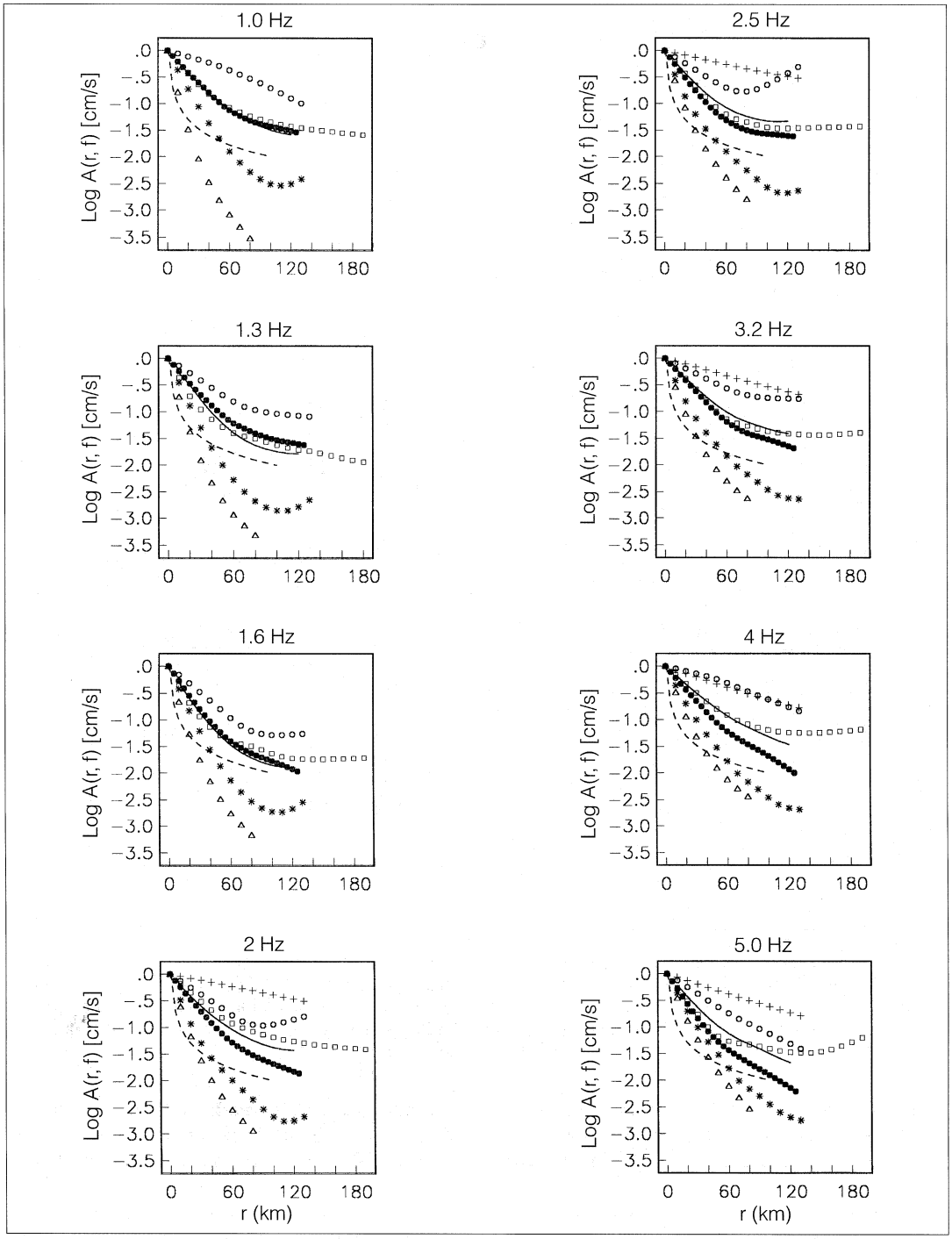
1.0 Hz
2.5 Hz
1.3 Hz
3.2 Hz
1.6 Hz
4 Hz
2 Hz
5.0 Hz
Log A(r, f) [cm/s]
.0
−.5
−1.0
−1.5
−2.0
−2.5
−3.0
−3.5
0
60
120
180
r (km)

Fig. 2.

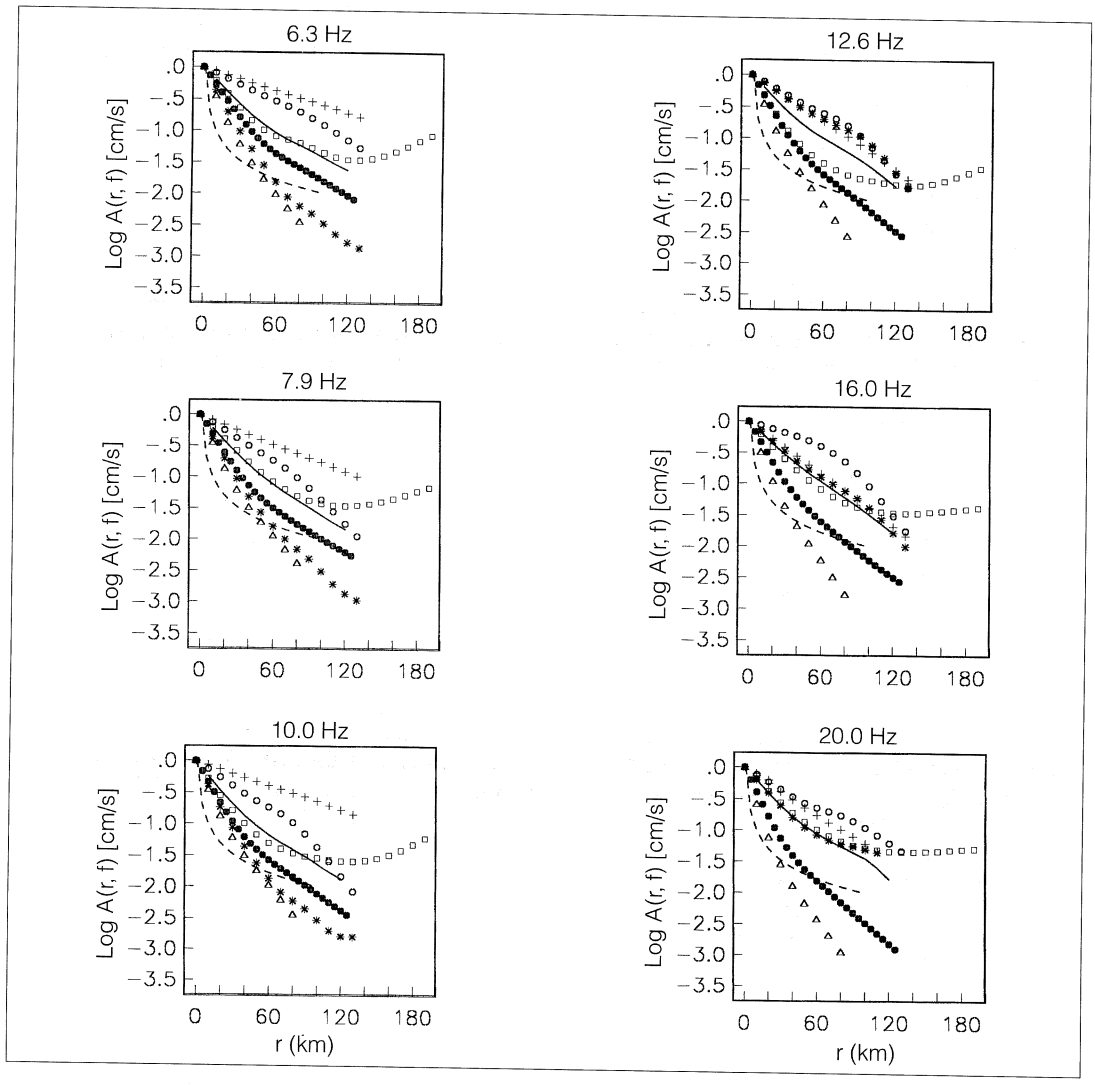

Fig. 2. Nonparametric Attenuation Functions (NAF) reported for the region of Lombardia (crosses), Piemonte-Lombardia (asterisks) and Eastern Sicily (circles). The squares represent the NAF obtained by Castro *et al.* (1996) for the region of Friuli, the black dots the functions reported for the region of Marche (Castro *et al.*, 1999a) and the triangles the NAF obtained by Castro *et al.* (1999b) for the Central Apennines. The continuous lines are the average calculated using the NAF of the first five regions.

For this region the NAF were calculated using seismograms from the Italian electricity board's (ENEL) local network of Viadana and the regional network of S. Benedetto Po. Most of the stations were located on the deep-alluvium filled Po plain, where the thickness of Quaternary sediments exceeds 1000 m. The characteristics of these networks are described by Bertuletti (1984). The earthquakes used were originated at the buried compressible fronts of the Northern Apennines and at the compressive folds of the Southern Alps. Six earthquakes with mag-

nitudes between 2.5 and 3.6 and hypocentral distances ranging between 23 and 125 km were selected from the region of Lombardia and another six events with distances ranging from 84 to 265 km and magnitudes between 2.8 and 4.0 from the region of Piemonte (Castro *et al.*, 1993). Two sets of NAF were obtained, one using data only from the region of Lombardia and another combining the data from the Lombardia-Piemonte region. In fig. 2 we plotted with crosses the NAF reported by Castro *et al.* (1993) for the region of Lombardia and with asterisks the functions obtained when the data of both regions were combined.

3.2. *Eastern Sicily*

The area studied (see fig. 1) is approximately coincident with the Iblean plateau, an undeformed carbonatic platform delimited northward by the Mount Etna volcano and eastward by the sedimentary Caltanissetta basin (Colombi *et al.*, 1973). Strong motion records from the December 13, 1990 earthquake (M 5.7) recorded by the ENEL accelerographic network were used to calculate the NAF of this region (Castro *et al.*, 1993). This data set consisted of the horizontal components of SMA-1 records digitized with an optical scanner (Rovelli *et al.*, 1991a; Di Bona *et al.*, 1995). The recording stations are located between 32 and 124 km of the hypocenter. Figure 2 shows with circles the NAF reported for Eastern Sicily.

3.3. *Friuli*

The Southern Alpine overthrust and the Dinaric overthrusts are the main tectonic structures of Friuli (Barbano *et al.*, 1985; Rovelli *et al.*, 1991b), and most thrust faulting earthquakes in this region are the result of the compressional regime of the Eastern Alps.

The data set used for the region of Friuli consists of 11 earthquakes recorded by the ENEL Accelerograph Network (Basili *et al.*, 1976) and the station Gemona del Friuli installed by the Istituto Nazionale di Geofisica (ING) during the 1976 earthquake sequence. A total of 180 horizontal component records from events with magnitudes between 4.2 and 6.4 were analyzed. The NAF obtained by Castro *et al.* (1996) using the strong motion records of this region are shown with squares in fig. 2.

3.4. *Marche*

The region of Marche extends towards the eastern side of the Northern Apennines. In this region gentle folds and thrusts composed of Pliocene-Pleistocene rocks are formed as a result of active compression, particularly in the Adriatic offshore (Ponziani *et al.*, 1995). The area considered covers the so-called external front of the Central Apennines, where the seismicity is the result of a tectonic regime mainly compressive.

Digital seismograms from 26 earthquakes recorded by the Marchesan Seismograph Network (RSM), jointly operated by the Geophysical Observatory of Macerata (OGSM) and the Italian Seismological Survey of Rome, were used by Castro *et al.* (1999a) to calculate NAF in this region. Most of the events used are located to the east of the Apenninic chain. The magnitude range is between 1.8 and 3.6, and the hypocentral distance range is between 9 and 125 km. The black circles in fig. 2 represent the NAF of the region of Marche.

3.5. *North-Central Apennines*

This region is part of the collisional plate boundary between Africa and Eurasia (Malinverno and Ryan, 1986). Extensional processes have also affected the Apennines and as a result of this graben-like structures have been formed trending N-S to NW-SE (Patacca and Scandone, 1987; Margheriti *et al.*, 1996). Most of the seismicity in this region is now normal-fault type, reversing the thrust mechanism trend that built up the Apenninic chain.

A set of horizontal-component records from 40 earthquakes located in the epicentral area of the Umbria-Marche sequence of 1997 and recorded by the digital stations of the RSM were used by Castro *et al.* (1999b) to calculate NAF

in the Central Apennines. The events which occurred two weeks before the main events of the sequence have magnitudes between 2.1 and 4.1 and hypocentral distances that range between 18 and 84 km. The triangles in fig. 2 represent the attenuation functions obtained for this region.

4. Discussion

When we compare the NAF from the different regions (fig. 2), distinct attenuation characteristics can be observed. For instance, while the Central Apennines show the strongest amplitude decay for all the frequencies analyzed, the *S* waves tend to attenuate less in the regions of Eastern Sicily and Lombardia. It is also interesting to note that the rate of decay is not constant for all the distance range. For Friuli, for example, the rate of decay changes near 60 km, flattening at distances greater than 100 km. This change in amplitude decay at long distances can be related to Moho reflections, the arrival of high-frequency *Lg* waves and other propagation-path effects (*e.g.*, Campillo *et al.*, 1984; Somerville and Yoshimura, 1990). Thus, the change of inflection of the NAF may be used to infer, qualitatively, differences of crust thickness among the regions studied. If we compare the Moho isobaths reported by Nicolich and Dal Piaz (1990) with the NAF shown in fig. 2, we can observe that the region of Piemonte-Lombardia, which has the thickest crust (40-50 km), also has a change of amplitude decay at a longer distance than the other regions, namely at 100 km. The other regions, that have a thinner crust, between 30 and 35 km (Nicolich and Dal Piaz, 1990; Alessandrini *et al.*, 1995), show the change of rate of amplitude decay at shorter distances (between 60 and 80 km).

In order to analyze the degree of significance of the differences of attenuation observed between the regions investigated, in fig. 3 we plotted the Root Mean Square (RMS) error determined for each NAF (one per frequency). To distinguish the different regions we used in fig. 3 the same symbols as in fig. 2. The RMS error takes the highest values for the Piemonte-Lombardia NAF for $f < 10$ Hz (asterisks). In general, the RMS error decreases with frequency up to about 15 Hz, then the error increases. The values of RMS shown in fig. 3 indicate that, in general, the differences in attenuation become significant only at long hypocentral distances ($r > 30$ km). It is also clear that for the regions of Marche and Friuli, which show similar amplitude decay, the difference of rate of decay is significant only at longer distances ($r > 60$ km) and high frequencies ($f > 5$ Hz).

The attenuation of *S* waves can also be correlated with the velocity of propagation. Thus, high attenuation may be expected where the waves travel through a low velocity zone (*e.g.*, Winkler and Nur, 1982). In order to explain the different rate of decay of the regions shown by the NAF (fig. 2), we can compare the velocity adjustments obtained by Alessandrini *et al.* (1995) from a crustal tomography study of Italy. In that study, a reference velocity model, based on previous models reported by Mantovani *et al.* (1980) and Mele and Valensise (1987), was first defined and then adjustments of the velocity parameters were found through a linearized 3D inversion. The results of this inversion show

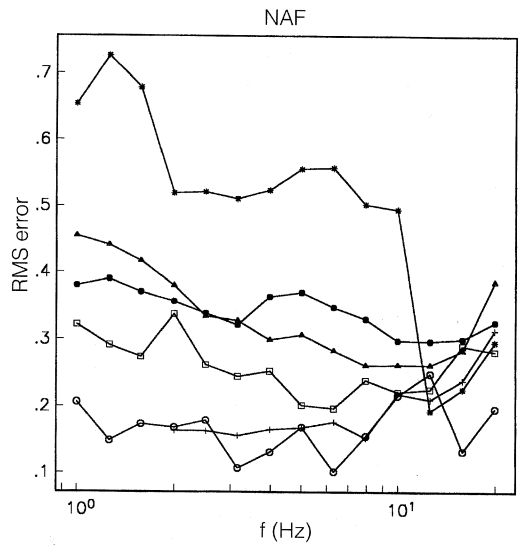

Fig. 3. Root mean square errors estimated for the NAF shown in fig. 2. We used the same symbols, as in fig. 2, to distinguish the different regions.

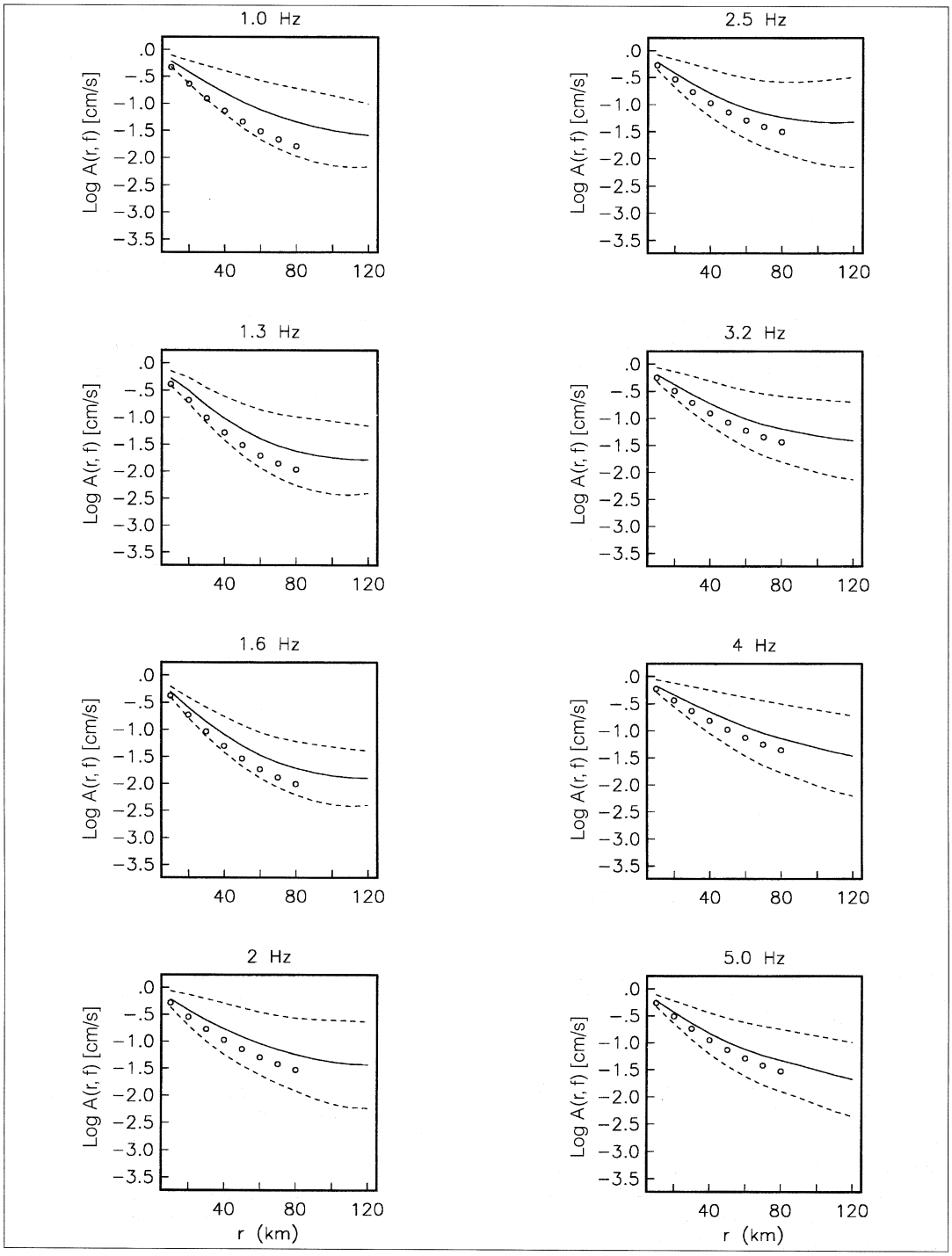
1.0 Hz
2.5 Hz
1.3 Hz
3.2 Hz
1.6 Hz
4 Hz
2 Hz
5.0 Hz
Log A(r, f) [cm/s]
.0
-.5
-1.0
-1.5
-2.0
-2.5
-3.0
-3.5
40
80
120
r (km)

Fig. 4.

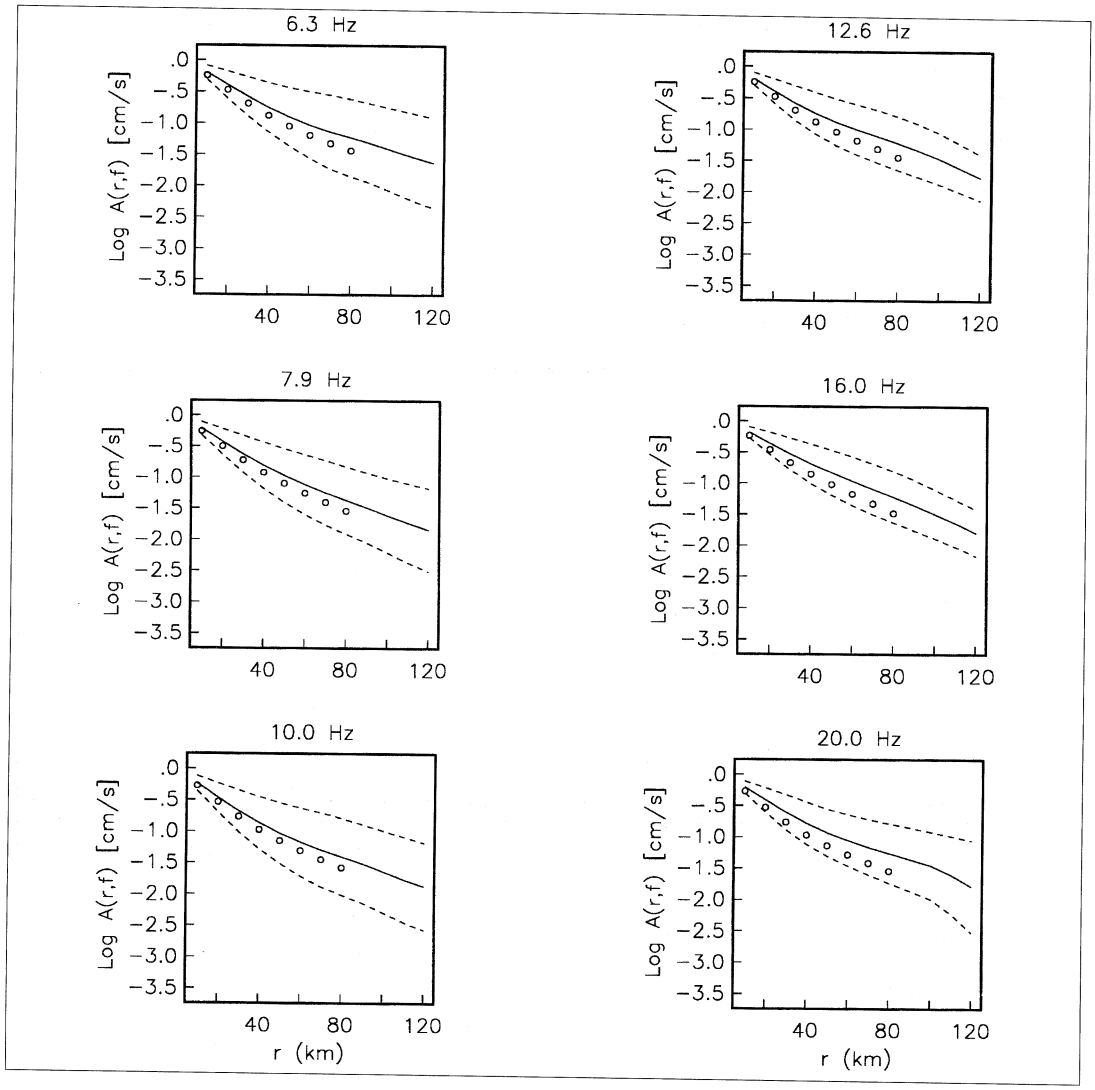

Fig. 4. Average attenuation functions (solid line) and their standard deviation (dashed lines) calculated using the NAF that extend from 10 km to 120 km (all functions shown in fig. 1 except those from the Central Apennines). The circles represent the average obtained using all the functions in the distance range from 10 to 80 km.

that the Apenninic chain is characterized by low velocity in its northern and central parts. This low velocity can be correlated with the high attenuation shown by the obtained NAF (triangles in fig. 2). In contrast, Alessandrini *et al.* (1995) reported high velocity values for the Western Alps and the regions of Friuli, Eastern Sicily and Marche, where the NAF indicated lower attenuation.

Since the attenuation functions shown in fig. 2 sample regions with different geologic and tectonic characteristics, an average set of NAF, representative for Italy, can be obtained. Figure 4 shows this average (solid line) and the stand-

Table I. Average attenuation functions (Log $\bar{A}(r, f)$) calculated using the NAF shown in fig. 2.

F (Hz)	10 km	20 km	30 km	40 km	50 km	60 km
1.00	–.21357	–.42332	–.61797	–.80035	–.97062	–1.12020
1.26	–.27766	–.50275	–.77975	–.10181	–.12240	–1.39765
1.58	–.30155	–.59380	–.85535	–.10883	–.12969	–1.47415
2.00	–.21408	–.41818	–.60274	–.76704	–.91240	–1.04144
2.51	–.21710	–.42526	–.61882	–.79494	–.94830	–1.07622
3.16	–.19512	–.38216	–.55924	–.72594	–.87804	–1.01376
3.98	–.17096	–.33774	–.49652	–.64782	–.78940	–0.92340
5.01	–.21946	–.43360	–.63762	–.82608	–.98706	–1.12340
6.31	–.19812	–.39210	–.57962	–.75296	–.90346	–1.03420
7.94	–.21514	–.42656	–.62740	–.81088	–.97438	–1.11962
10.00	–.23666	–.46702	–.67916	–.86836	–.10332	–1.17496
12.59	–.19954	–.39638	–.58162	–.74568	–.88654	–1.00416
15.85	–.17980	–.35910	–.53064	–.68712	–.82976	–0.96352
19.95	–.20556	–.41046	–.60568	–.78026	–.92956	–1.05310

ard deviation (dashed lines) calculated using the NAF that extend from 10 km to 120 km (all functions except those from the Central Apennines). Figure 4 also shows, with circles, the average obtained from 10 to 80 km using all the functions. The latter functions (plotted with circles) are inside the standard deviation of the average calculated from 10 to 120 km. However, to avoid a discontinuity of the attenuation curves at 80 km we decided to calculate separate averages, one set between 10 and 120 km (solid lines) and another set between 10 and 80 km. Table I lists the average values of Log $A(r, f)$ obtained with the NAF that extend from 10 to 120 km for the 14 frequencies analyzed ($1 \leq f < 20$ Hz). The continuous lines in fig. 2 are the average NAF, which provide a reference frame of comparison. In fig. 2 we also plotted, with dashed lines, the amplitude decay corresponding to $1/r$. Note that at short distances ($r < 20$ km) and $f > 2$ Hz the NAF of the Central Apennines (triangles) approximately follow the $1/r$ decay.

Although a standard $1/r$ amplitude decay is usually adopted to describe the amplitude decay of body waves, recent studies show that a less steep spreading function can be more adequate. For instance, Olafson *et al.* (1998) found that a spreading function $1/r^{0.65}$ better fits observed strong-motion records in South Iceland. Castro *et al.* (1999a) model the spreading function in the region of Marche using a functional form given by $G(r) = c/r^n$ and found an average value of $c = 3.86$ and $n = 0.81$ for *SH* waves. The main advantage of using NAF to characterize the spectral amplitude decay is that it is not necessary to adopt any parametric function to describe the spreading function, since this and other attenuation effects are implicitly included in the NAF.

In fig. 5 we compare the amplitude decay of a sample of average NAF for the frequency band between 2 and 16 Hz. It is interesting to note that at low frequencies ($f < 5$ Hz), where the *S*-wave lengths are longer and the surface waves begin to have a stronger effect on the spectral amplitudes, a change in rate of amplitude decay can be observed between 60 and 80 km. At higher frequencies ($f \geq 7.9$ Hz) the change in rate of decay is less pronounced.

To illustrate the use of the average NAF listed in table I, we calculated acceleration spec-

70 km	80 km	90 km	100 km	110 km	120 km
–1.24347	–1.34640	–1.43085	–1.49857	–1.55035	–1.58652
–1.53052	–1.62685	–1.69577	–1.74635	–1.77735	–1.78445
–1.61047	–1.71462	–1.79517	–1.85360	–1.88685	–1.89660
–1.15192	–1.24358	–1.32082	–1.38056	–1.41872	–1.43436
–1.17442	–1.24340	–1.29506	–1.32904	–1.34060	–1.32948
–1.12080	–1.19954	–1.26650	–1.32830	–1.37906	–1.41728
–1.04150	–1.13804	–1.22516	–1.31306	–1.39448	–1.46314
–1.23686	–1.32656	–1.41214	–1.50506	–1.59654	–1.67634
–1.14498	–1.23538	–1.32684	–1.43124	–1.53596	–1.62964
–1.25142	–1.37314	–1.49076	–1.61448	–1.73456	–1.84192
–1.29866	–1.40698	–1.51616	–1.64052	–1.76684	–1.87678
–1.11212	–1.22220	–1.33812	–1.46914	–1.61592	–1.77012
–1.09322	–1.22104	–1.35132	–1.49116	–1.63868	–1.78952
–1.16052	–1.25878	–1.35336	–1.44930	–1.59953	–1.78590

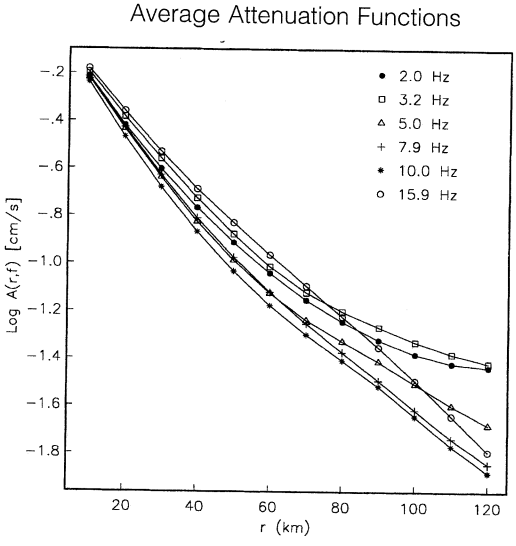

Fig. 5. A comparison of average NAF obtained in the distance range between 10 and 120 km. The black dots represent the average function for 2.0 Hz, the squares for 3.2 Hz, the triangles for 5 Hz, the crosses for 7.9 Hz and the circles for 15.9 Hz.

tra predicted by the Brune (1970) model and then we added the attenuation effect. Thus, the attenuated spectra can be expressed as

$$u(r,f) = \ddot{M}_0(f) \cdot \overline{A}(r,f) \tag{4.1}$$

where $\overline{A}(r,f)$ is the average attenuation function for distance r and frequency f as listed in table I and

$$\ddot{M}_0(f) = \frac{C \cdot M_0}{r} \frac{\omega^2}{1 + \left(\frac{\omega^2}{\omega_c^2}\right)} \tag{4.2}$$

is the acceleration source function (Brune, 1970), were M_0 is the seismic moment, $\omega = 2\pi f$, ω_c is the corner frequency and the constant C is given by

$$C = \frac{0.6}{4\pi\rho\beta^3} \tag{4.3}$$

we used a value of ρ = 2.9 gr/cm^3 and β = 3.2 km/s.

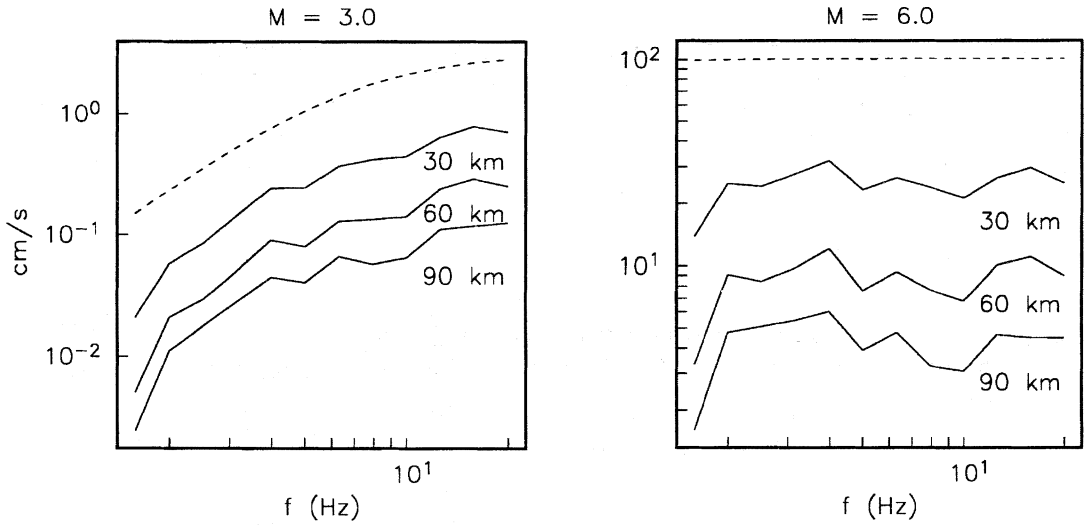

Fig. 6. Acceleration spectra calculated with the ω^2 model (Brune, 1970) using a constant stress drop of 30 bars. The curves on the left frame were calculated using a seismic moment equivalent to $M = 3.0$ and the curves on the right using a M_0 equivalent to $M = 6.0$. The dashed lines are the acceleration source functions and the solid lines the source spectra multiplied by the corresponding NAF (table I).

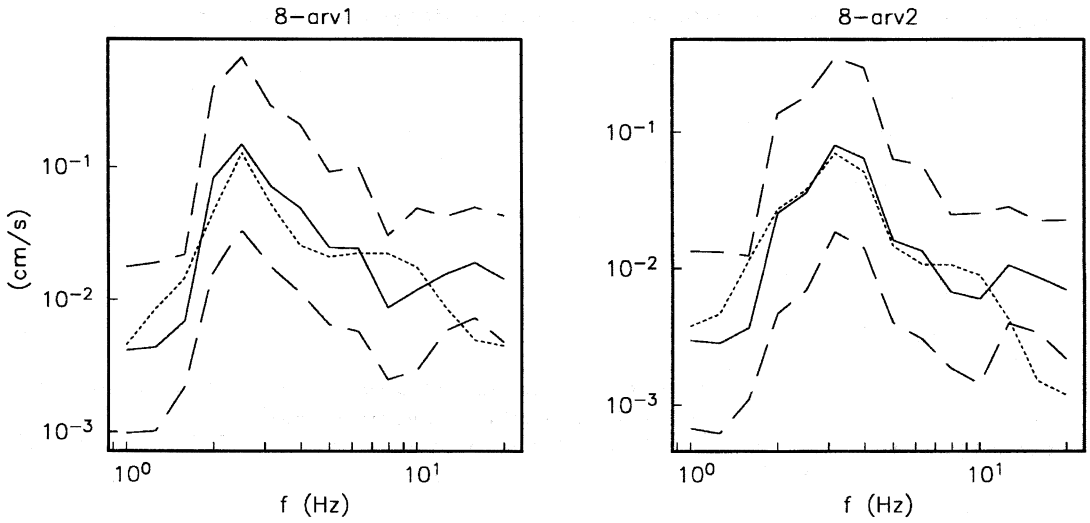

Fig. 7. Acceleration spectra observed (dots) on top of Arvo lake (left frame) and on the free-field (right frame). The continuous lines are the spectra calculated with Brune's model for M_L 3, corner frequency 2 Hz, the NAF corresponding to 90 km (table I) and the site functions reported by Castro *et al.* (1998) for the recording sites. The dashed lines represent the upper and lower bounds of the estimates.

Figure 6 shows acceleration spectra calculated with the model of Brune (1970) for an equivalent magnitude M = 3.0 (left frame) and for M = 6 (right frame), using a constant stress drop of 30 bars. The dashed lines are the acceleration source functions calculated with eq. (4.2) and the solid lines the acceleration spectra calculated with eq. (4.1) using the average attenuation functions listed in table I. Since the attenuation functions contain implicitly the effect of both Q and geometrical spreading, we fit r = 1 km in eq. (4.2). It is also important to point out that in eq. (4.1) the site effects have not been taken into account to estimate the spectral amplitudes. For M = 3 the corner frequency of the spectra, for the stress drop used, is at 7.15 Hz. However, for M = 6 the corner frequency is at 0.23 Hz, outside the frequency band of the NAF. In spite of this, fig. 6 illustrates the effect of the attenuation on the high-frequency acceleration spectra for three different distances (30, 60 and 90 km). Thus, it is interesting to note that for M = 6 the attenuation can diminish the spectral amplitudes from 30 to 60 km by a factor of approximately 3 times and from 60 to 90 km by a factor of 2. This illustrates the nonlinear effect of the attenuation on the spectral amplitudes.

In order to test the reliability of the average NAF obtained, we selected a pair of sites located in the region of Calabria, where there is no NAF available, to estimate the acceleration spectra. One of the sites (ARV1) is located on top of an earth dam, in Arvo lake, and the other site (ARV2) is on free field near the dam. For these two sites Castro *et al.* (1998) found the site response using a spectral inversion technique. Thus, we can add the site effect of these sites to the acceleration spectra estimated with eq. (4.1).

The dots in fig. 7 represent the observed acceleration spectra (square root of the product of the two horizontal components) from an M_L = 3 earthquake located approximately at 90 km of the dam. The continuous line is the spectrum calculated using a corner frequency of 2 Hz, and the dashed lines the upper and lower error bounds estimated from the standard deviation of the average NAF. In fig. 7 the observed spectrum is inside the error of the estimate for most of the frequency band considered. However, at high frequencies (f > 12 Hz) the average attenuation (table I) overestimates the spectral amplitudes. It is possible that in the region of Calabria the attenuation is stronger for that frequency band (f >12 Hz) or that the site effects were overestimated. In any case, the average attenuation and the site responses used approximate the maximum spectral amplitudes reasonably well.

5. Conclusions

We calculated a set of average attenuation functions for the Italian region using nonparametric functions published in previous studies (fig. 3 and table I). These average functions provide a conservative attenuation correction in the frequency band $1.0 \leq f < 20$ Hz for source-receiver distances between 10 and 120 km. These functions can be useful to make a mean attenuation correction in regions where the specific attenuation parameters are unknown. The average NAF obtained also give a reference frame of comparison. Thus, while Central Apennines show high attenuation (above the average) for all the frequencies analyzed, the regions of Eastern Sicily and Lombardia show low attenuation (see fig. 2). The region of Marche also shows attenuation above the average for $f \geq 2.0$ Hz and the region of Friuli for $f \geq 12.6$ Hz. In the frequency band $1 \leq f < 3$ Hz, the S-wave attenuation of the regions of Friuli and Marche is similar. The NAF of the Piemonte-Lombardia region show high attenuation up to 10.0 Hz, then the attenuation becomes above average as in the region of Lombardia.

Acknowledgements

This work was partially supported by the *Consiglio Nazionale delle Ricerche*. The manuscript was written while one of the authors (RRC) was visiting the OGSM and the ING-Roma. We acknowledge Prof. Roberto Murri and the partial support of the Mexican National Council of Science and Technology (CONACYT). We thank Alfio Sala, Pietro Caroli, Luca Trojani, Massimo Frapiccini, Henry Coppary and Viviana Castelli for the help provided during the analysis of the data. We are grateful to Antonio Rovelli and the anonymous reviewer for their comments.

REFERENCES

ALESSANDRINI, B., L. BERANZOLI and F.M. MELE (1995): 3D crustal *P*-wave velocity tomography of the Italian region using local and regional seismicity data, *Ann. Geofis.*, **38** (2), 189-211.

ANDERSON, J.G. and Y. LEI (1994): Nonparametric description of peak acceleration as a function of magnitude, distance and site in Guerrero, Mexico, *Bull. Seismol. Soc. Am.*, **84**, 1003-1017.

ANDERSON, J.G. and R. QUAAS (1988): The Mexico earthquake of September 19, 1985: effect of magnitude on the character of strong ground motion: an example from the Guerrero, Mexico strong motion network, *Earthquake Spectra*, **4**, 635-646.

BARBANO, M.S., R. KIND and G. ZONNO (1985): Focal parameters of some Friuli earthquakes (1976-1979) using complete theoretical seismograms, *J. Geophys.*, **58**, 175-182.

BASILI, M., R. BERARDI, F. MUZZI, S. POLINARI, G. TINELLI and L. ZONETTI (1976): Strong motion records relative to the Friuli earthquake accelerogram processing and analysis, Osservatorio Geofisico Sperimentale, Trieste, Italy, *Bull. Geofis.*, **19**, 335-348.

BERTULETTI, O. (1984): Rete di rilevamento della sismicità locale a S. Benedetto Po, *Rapporto Finale, ISMES*, practica n. 2208, doc. n. RAT-DGF-0007.

BRILLINGER, D.R. and H.K. PREISLER (1984): An exploratory analysis of the Joyner-Boore attenuation data, *Bull. Seismol. Soc. Am.*, **74**, 1441-1450.

BRUNE, J.N. (1970): Tectonic stress and the spectra of seismic shear waves from earthquakes, *J. Geophys. Res.*, **75**, 4997-5009.

CAMPILLO, M., M. BOUCHON and B. MASSINON (1984): Theoretical study of the excitation, spectral characteristics and geometrical attenuation of regional seismic phases, *Bull. Seismol. Soc. Am.*, **74**, 79-90.

CASTRO, R.R., J.G. ANDERSON and S.K. SINGH (1990): Site response, attenuation and source spectra of *S* waves along the Guerrero, Mexico, subduction zone, *Bull. Seismol. Soc. Am.*, **80**, 1481-1503.

CASTRO, R.R., F. PACOR and C. PETRUNGARO (1993): Confronto fra diversi metodi per la stima dell'attenuazione delle onde sismiche applicati nelle regioni Lombardia e Sicilia, in *Atti del 12° Convegno, Consiglio Nazionale delle Ricerche, Gruppo Nazionale di Geofisica della Terra Solida,* 179-192.

CASTRO, R.R., F. PACOR, A. SALA and C. PETRUNGARO (1996): *S* wave attenuation and site effects in the region of Friuli, Italy, *J. Geophys. Res.*, **101**, 22355-22369.

CASTRO, R.R., M. MUCCIARELLI, F. PACOR, P. FEDERICI and A. ZANINETTI (1998): Determination of the characteristic frequency of two dams located in the region of Calabria, Italy, *Bull. Seismol. Soc. Am.*, **88**, 503-511.

CASTRO, R.R., G. MONACHESI, M. MUCCIARELLI, L. TROJANI and F. PACOR (1999a): *P* and *S*-wave attenuation in the region of Marche, Italy, *Tectonophysics*, **302**, 123-132.

CASTRO, R.R., G. MONACHESI, L. TROJANI, M. MUCCIARELLI and M. FRAPICCINI (1999b): An attenuation study using earthquakes from the 1997 Umbria-Marche sequence (submitted).

COLOMBI, B., P. GIESE, G. LUONGO, C. MORELLI, M. RIUSCETTI, S. SCARASCIA, K.G. SCHUTTE, J. STROWALD and G. DE VISINTINI (1973): Preliminary report on the seismic refraction profile Gargano-Salerno-Palermo-Pantelleria (1971), *Boll. Geofis. Teor. Appl.*, **15**, 225-252.

DI BONA, M., M. COCCO, A. ROVELLI, R. BERARDI and E. BOSCHI (1995): Analysis of strong-motion data of the 1990 Eastern Sicily earthquake, *Ann. Geofis.*, **38** (2), 283-300.

MALINVERNO, A. and W.B.F. RYAN (1986): Extension in the Tyrhenian Sea and shortening in the Apennines as a result of arc migration driven by sinking of lithosphere, *Tectonics*, **5**, 227-246.

MANTOVANI, E., F. FARSI and D. BABBUCCI (1980): Body wave velocities and lateral heterogeneity in the Italian region, *Boll. Geofis. Teor. Appl.*, **22**, 211-221.

MARCHANT, R.H. (1993): The underground of the Western Alps, *Mem. Geol.* (Lausanne), **15**, pp. 137.

MARGHERITI, L., C. NOSTRO, M. COCCO and A. AMATO (1996): Seismic anisotropy beneath the Northern Apennines (Italy) and its tectonic implications, *Geophys. Res. Lett.*, **23**, 2721-2724.

MELE, F.M. and G. VALENSISE (1987): Un modello crostale per la localizzazione di eventi sismici regionali rilevati dalla Rete Sismica Nazionale Centralizzata dell'ING, in *Proceedings of the 6° Annual Meeting of the Gruppo Nazionale di Geofisica della Terra Solida*, Roma, Italy, 1377-1395.

NICOLICH, R. and R. DAL PIAZ (1990): Moho isobaths, in *Structural Model of Italy and Gravity Map, Sheet 2*, Consiglio Nazionale delle Ricerche.

OLAFSON, S., R. SIGBJORNSSON and P. EINARRSON (1998): Estimation of source parameters and *Q* from acceleration recorded in the Vatnafjoll earthquake in Southern Iceland, *Bull. Seismol. Soc. Am.*, **88**, 556-563.

PATACCA, E. and P. SCANDONE (1987): Segmentation and configuration of subducted lithosphere in Italy: an important control on thrust-belt and foredeep-basin evolution, *Geology*, **25**, 714-717.

PONZIANI, F., R. DE FRANCO, G. MINELLI, G. BIELLA, C. FEDERICO and G. PIALLI (1995): Crustal shortening and duplication of the Moho in the Northern Apennines: a view from seismic refraction data, *Tectonophysics*, **252**, 391-418.

ROVELLI, A., E. BOSCHI, M. COCCO and M. DI BONA (1991a): Il terremoto del 13 dicembre 1990 nella Sicilia Orientale: analisi dei dati accelerometrici, in *Publication of Istituto Nazionale di Geofisica* No. 537, 85-101.

ROVELLI, A., M. COCCO, R. CONSOLE, B. ALESSANDRINI and S. MAZZA (1991b): Ground motion waveforms and source spectral scaling from close-distance accelerograms in a compressional regime area (Friuli, Northeastern Italy), *Bull. Seismol. Soc. Am.*, **81**, 57-80.

SOMERVILLE, P. and J. YOSHIMURA (1990): The influence of critical Moho reflections on strong ground motions recorded in San Francisco and Oakland during the 1989 Loma Prieta earthquake, *Geophys. Res. Lett.*, **17**, 1203-1206.

SPAKMAN, W., S. VAN DER LEE and R. VAN DER HILST (1993). Travel time tomography of the European Mediterranean-mantle down to 1400 km, *Phys. Earth Planet. Inter.*, **79**, 3-74.

WINKLER, K.W. and A. NUR (1982): Seismic attenuation: effects of pore fluids and frictional sliding, *Geophysics*, **47**, 1-15.

(received March 12, 1999;
accepted July 2, 1999)